Desalination and Water Treatment
www.deswater.com

doi: 10.5004/dwt.2021.27159

223 (2021) 447–455
May

Performance of self-cleaning cotton textiles coated with TiO_2, TiO_2-SiO_2 and TiO_2-SiO_2-HY in removing Rhodamine B and Reactive Red 120 dyes from aqueous solutions

Salmon Landi Jr.[a,b,*], Joaquim Carneiro[a], Pier Parpot[c,d], Olívia S.G.P. Soares[e], Manuel F.R. Pereira[e], António M. Fonseca[c,d], Isabel C. Neves[c,d]

[a]*Centre of Physics, University of Minho, Azurém Campus, Guimarães 4800-058, Portugal, emails: salmon.landi@ifgoiano.edu.br (S. Landi Jr.), carneiro@fisica.uminho.pt (J. Carneiro)*
[b]*Instituto Federal Goiano, 75901-970, Rio Verde, Goiás, Brazil*
[c]*CEB, Centre of Biological Engineering, University of Minho, Gualtar Campus, Braga, 4710-057, Portugal, emails: parpot@quimica.uminho.pt (P. Parpot), amcf@quimica.uminho.pt (A.M. Fonseca), ineves@quimica.uminho.pt (I.C. Neves)*
[d]*CQUM, Centre of Chemistry, Chemistry Department, University of Minho, Gualtar Campus, Braga 4710-057, Portugal*
[e]*Laboratory of Catalysis and Materials – Associate Laboratory LSRE/LCM, Faculty of Engineering, University of Porto, 4200-465 Porto, Portugal, emails: salome.soares@fe.up.pt (O.S.G.P. Soares), fpereira@fe.up.pt (M.F.R. Pereira)*

Received 10 March 2020; Accepted 18 February 2021

ABSTRACT

In the present study composites based on TiO_2 nanoparticles, SiO_2 and HY zeolite were synthesized by using a standard sol-gel methodology and analyzed by Fourier-transform infrared spectroscopy, X-ray diffraction and scanning electron microscopy-energy-dispersive X-ray spectroscopy techniques. The photocatalysts were impregnated on cotton textiles and their photocatalytic abilities were examined by degradation of Rhodamine B (RhB) and Reactive Red 120 (RR120) dyes in aqueous solution under similar solar irradiation. RhB removal efficiencies from cotton textiles were 87%, 72% and 50% for TiO_2, TiO_2-SiO_2-HY zeolite and TiO_2-SiO_2 composites, respectively and achieved after 3 h of light irradiation. However, for the RR120 dye, the reached result was different as the photodegradation for this dye (65% efficiency) was only observed in bare TiO_2 functionalized textile. In addition, for the treatment with TiO_2-SiO_2-HY zeolite, it was found that for initial alkaline conditions at pH of the RhB dye solution, the photodegradation rate decreased.

Keywords: TiO_2, Photocatalysis; Environmental remediation; RhB dye; Reactive Red 120 dye

1. Introduction

Since the pioneering works published in the 1960s [1], photocatalysis based on semiconductor materials has been widely applied for environmental remediation not only for fundamental research [2–8] but also in pilot projects [9–11]. This phenomenon is related to the structure of semiconductor electronic bands and the potential of oxidation and reduction of the target molecules. Currently, the literature shows that several aquatic contaminants, such as, fungicides, herbicides, pesticides, phenols, pigments, dyes, detergents, antibiotics, contraceptives, estrogens, among others, can be destroyed by a sequence of redox reactions that take place on the semiconductors surface under ultraviolet and/or visible light. In general, photodegradation rates depend on the pollutant nature, initial pH, concentration of different species dissolved in the treated solution, wavelength and irradiance of the incident light, as well as the surface

* Corresponding author.

area, morphology, particle size and crystallinity of the semiconductor material [12].

Due to the presence of oxygen vacancies, titanium dioxide (TiO_2) is an intrinsically *n*-type semiconductor material [13] with an energy bandgap equal to 3.2 eV (anatase crystalline phase – indirect allowed transition) and 3.0 eV (rutile crystalline phase – direct allowed transition) [14]. Therefore, the production of an electron in its conduction band and hole in its valence band requires the absorption of a photon with energy in the UV region of the electromagnetic spectrum. These generated charge carriers are responsible for the formation of free radicals that start the degradation process (without selectivity) of undesirable molecules in water [15–17] and air [18,19]. Although, only about 5% of the sunlight that reaches the earth' surface has enough energy to activate TiO_2 [20,21], that is, in the UV region, even so, TiO_2 is still the most attractive semiconductor in the heterogeneous photocatalysis for degradation of toxic organic compounds in water [22]. This fact is mainly due to its highly desirable characteristics such as being inexpensive, biologically and chemically inert, nontoxic and also presenting tuneable properties (bandgap, particle size, crystallinity and others) [23–25].

It should be emphasized that much work has been performed in order to obtain TiO_2-based materials even more efficiently than just this bare semiconductor. Namely, SiO_2 is usually utilized to enhance textural and structural properties [26,27]. Under this context, the synthesis of composites based on SiO_2 and TiO_2 gives rise to a material with a larger surface area compared to the bare TiO_2 [28] and, at the same time, the presence of SiO_2 may inhibit the formation of rutile phase [29], which, in general, presents a lower photocatalytic efficiency compared to the anatase phase [30]. On the other hand, zeolites (crystalline microporous aluminosilicate consisting of SiO_4 and AlO_4^- tetrahedrons [31]) also comprise a class of materials commonly associated with TiO_2. In such cases, the presence of active sites in the zeolites may act as TiO_2 support, decrease the recombination of electron/hole pairs, bring the organic molecules closer to the photocatalyst surface [32], or even providing the formation of free radical due to the existence of Brønsted and Lewis acid sites in these structures [33].

It is well-known that in water treatment, suspended powders tend to form aggregates so their separation from the liquid state and the corresponding recycling process is problematic. The penetration depth of sunlight is limited due to the strong absorption by the suspended catalyst powders and dissolved organic substances. These difficulties can be overcome by immobilizing the catalyst particles on inert surfaces, such as cotton substrates, activated carbon fiber, cement surface, etc. Here, the choice fell on the cotton substrate since it is a light and inert material, flexible (therefore easily adaptable to different reactor geometries used in water treatment systems), easily available on the market (especially when applied in large areas) and inexpensive. Therefore, the immobilization of photocatalysts on inert supports (such as the cotton material) opens the possibility of catalyst recycling, thus reducing the costs associated with the long settling times or filtration methods for its recovery.

In this work, Rhodamine B (RhB) and Reactive Red 120 (RR120) dyes (Fig. 1) have been selected as pollutant models due to their wide use in the textile industry according to [34,35], respectively. Besides that, while RhB is a cationic dye, the RR120 dye has anionic character. In this sense, the main goal of the present study is to report and explain the decrease in the concentration of aqueous solutions of RhB and RR120 dyes in contact with cotton textiles coated with TiO_2, TiO_2-SiO_2 and TiO_2-SiO_2-HY zeolite photocatalysts.

2. Experiments

2.1. Materials

Bleached cotton textiles of 5 cm × 5 cm were plentifully washed using non-ionic detergent to remove any impurities and dried at room temperature before starting the functionalization process. TiO_2 nanoparticles (80% anatase and 20% rutile) were purchased from Quimidroga Portugal Lda. (Lisboa, Portugal). Commercially available HY zeolite (CBV 400, Si/Al = 2.81, already in the acidic form) was obtained from Zeolyst International Inc., (Pennsylvania, USA). Tetraethyl orthosilicate (TEOS, $Si(OC_2H_5)_4$, Sigma-Aldrich, Merck Life Science S.L.U. Branch in Portugal, Algés, Portugal) was employed as a precursor for SiO_2. Ethanol (from Merck S.A., Algés, Portugal) and distillate water were utilized as solvents and ammonium hydroxide (NH_4OH, from Sigma-Aldrich, Merck Life Science S.L.U. Branch in Portugal, Algés, Portugal) was used as a catalyst for hydrolysis reactions.

2.2. Photocatalysts preparation and coating processes

Initially, the composites used for the functionalization process of the cotton textiles were prepared according to

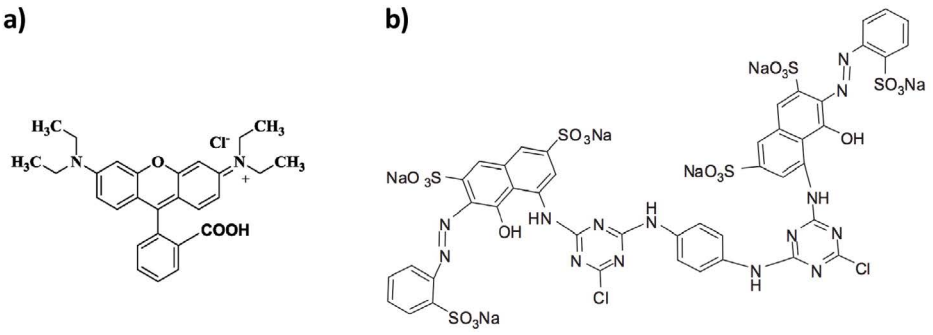

Fig. 1. Molecular structure of (a) Rhodamine B (RhB) and (b) Reactive Red 120 (RR120).

the procedure reported by Díaz et al. [36]. Succinctly, the hydrolysis of TEOS (2.30 g) was accomplished by the TiO_2 nanoparticles (0.70 g), ethanol (1.20 mL) and distilled water (1.00 mL) in an alkaline medium (20 μL of NH_4OH). Next, the HY zeolite was added (in order to obtain 30% by weight of the sum of TEOS precursor and TiO_2 nanoparticles) in the refluxed solution, which was magnetically stirred for 6 h at 70°C. The application of the reflux technique promotes the hydrolysis of TEOS, the condensation of reagents and the return of this condensate to the system, allowing a better reaction yield, with no loss of reagents or products by evaporation. The obtained gel was dried at 70°C in an oven for 24 h. The composite particles were ground in a mortar and then used in the preparation of suspensions to be applied in the functionalization of cotton textiles by a dip-coating process, according to Xu et al. [37]. Regarding the immobilization procedure, the pre-cleaned cotton samples remained for 1 min in a suspension (30 mg photocatalyst and 30 mL of methanol) previously sonicated for 5 min and then dried at room temperature. The immersion of the samples in the suspension was repeated three times and afterward the samples were cured at 100°C for 10 min.

2.3. Characterization

The crystalline phases and structural properties of TiO_2 and prepared composites were analyzed by X-ray diffraction (XRD) data (Bruker D8 DISCOVER, Agilent, Santa Clara, USA) obtained from Cu Kα radiation (λ = 1.54056 Å). Fourier-transform infrared (FTIR) spectra were acquired via a Bomem MB-104 spectrometer (ABB Bomem Inc., Quebec, Canada) with a resolution of 4 cm^{-1}, in the transmittance mode by using 32 scans. For this purpose, pellets were prepared by mixing the photocatalysts with KBr (1% by wt. photocatalyst – 99% by wt. KBr). Electrokinetic behavior of TiO_2, TiO_2-SiO_2 and TiO_2-SiO_2-HY aqueous suspensions was studied by zeta potential measurements in a pH range between 2 and 10 (Zetasizer NS 2007). Textural properties were calculated from the analysis of N_2 adsorption–desorption isotherms measured at –196°C with a Nova 4200e (Quantachrome Instruments, Florida, USA) equipment. The micropore volumes (V_{micro}) and mesopore surface areas (S_{meso}) were calculated by the *t*-method. Surface areas were calculated by applying the Brunauer–Emmett–Teller equation. In order to observe the surface morphology of cotton fibers coated with different photocatalysts, scanning electron microscopy (SEM) was used. The same equipment (FEI Nova 200 FEG-SEM) was also employed to perform a quantitative analysis of the chemical composition of photocatalysts through energy-dispersive X-ray spectroscopy (EDX) technique.

2.4. Photocatalytic activity assessment

The photocatalytic activity of the cotton samples was investigated by the degradation of RhB and RR120 aqueous solutions through the following procedure. Firstly, the cotton samples were inserted in beakers along with 20 mL of dye aqueous solution and then sealed with a flexible film to prevent evaporation of the solution. Then, the cotton samples (within the beakers) were placed under a 300 W lamp (ULTRA-VITALUX E27) at a distance of about 30 cm. The solutions remained in contact with cotton samples for 1 h in the dark and 3 h under similar sunlight irradiation without any type of stirring process. During the 4 h, aliquots were withdrawn at specific time intervals and centrifuged at 6,000 rpm for 10 min. The absorbance of the obtained supernatant was measured by spectrophotometry (Shimadzu 3101PC) in the range of 300–700 nm and its maximum value was considered in the calculation of the solution's concentration. Once the absorbance measurements were completed, the supernatants were re-inserted into the beakers and the lamp was turned on again.

3. Results and discussions

The XRD patterns of HY zeolite and also of the synthesized composites are depicted in Fig. 2. XRD diffractogram of the TiO_2-SiO_2 composite shows the peaks of anatase and rutile phases, as can be identified from the JCPDS data files No. 21–1272 and 21–1276, respectively. Additionally, one can observe a very broad peak centered at 2θ = 23° (highlighted by arrow), which can be ascribed to the amorphous SiO_2 phase [38]. Also, the powder XRD patterns reveal characteristic peaks of the HY zeolite and the anatase and rutile phases of titanium in the TiO_2-SiO_2-HY composite. In addition, the HY unit cell dimension, *a* (cubic structure), was calculated from the values of the (533), (642), and (555) reflection peaks according to the ASTM D 3942-80 method [39]. Subsequently, the determined value for a_0 (obtained from averaging the three values of a_0 calculated from each of the three reflection peaks mentioned above) was used in Breck and Flanigen equation in order to calculate the number of Al atoms in the HY unit cell [40]. In addition, for faujasite zeolite, the total number of Si and Al atoms present in a unit cell is equal to 192, thus allowing the evaluation of the Si/Al ratio. The obtained identical values (Si/Al = 4.0 ± 0.6) for both HY and TiO_2-SiO_2-HY suggest that the zeolite structure in the composite is preserved. On the other hand, similarly to what is reported in other studies [39,41], this value is higher than the expected one (2.81), evidencing superposition effects of non-framework species [42].

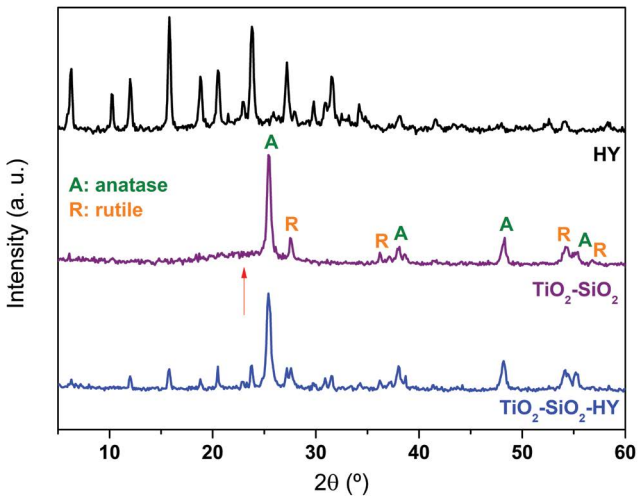

Fig. 2. X-ray diffraction pattern for HY zeolite and for the prepared composites.

FTIR spectrum of HY zeolite and the prepared composites are plotted in Fig. 3. A very broad band, observed in all spectra around 3,415 cm^{-1}, is related to the stretching vibration mode of surface silanol groups (Si–OH) and O–H bounds [43]. All the analyzed samples also present a peak at around 1,640 cm^{-1}, which is characteristic of the deformation mode of water [44]. The peaks at 3,160 cm^{-1} (marked with an asterisk) and 1,400 cm^{-1} in the spectrum of TiO_2-SiO_2-HY composite can be ascribed to the bending vibration mode of Si–CH_3 and O–H bonds, respectively [45]. These two peaks have been found to disappear after the composite has been heat-treated at 500°C for 5 h (data not shown), indicating that they probably correspond to the groups coming from the solvents (water and ethanol) used in the composite preparation. The located band around 1,090 cm^{-1} (common to spectra) is assigned to the Si–O–Si asymmetric stretching vibration [46]. The absorption peak related to the existence of Si–O–Ti bonds (at 953 cm^{-1} [37] and highlighted by an arrow) becomes more noticeable only for the composite without HY zeolite. Probably, this is because there is an overlap between this peak and an intense peak from the HY zeolite for the spectra of TiO_2-SiO_2-HY composite. Furthermore, the band observed between 600 and 570 cm^{-1} is often used to calculate the Si/Al ratio of the framework of faujasite zeolites and as has been discussed in our previous work [47]. Thus, considering the uncertain (2 cm^{-1}), the obtained values 580 cm^{-1} (TiO_2-SiO_2-HY) and 577 cm^{-1} (HY) share the same range, therefore their respective Si/Al ratios are also very similar 2.7 ± 0.2 and 2.9 ± 0.2. These negligible shifts indicate that the original structures of the HY zeolite remain unchanged, which is in agreement with the XRD results. It is important to note that, unlike by XRD results, this band is not influenced by non-framework species and, for this reason, the value obtained from FTIR measurements is lower than that calculated by XRD [42].

Fig. 4 shows SEM images of the HY zeolite and TiO_2 nanoparticles used in the preparation of the composites. The average particle size of the HY particles and TiO_2 nanoparticles is 400 ± 10 nm and 40 ± 7 nm, respectively.

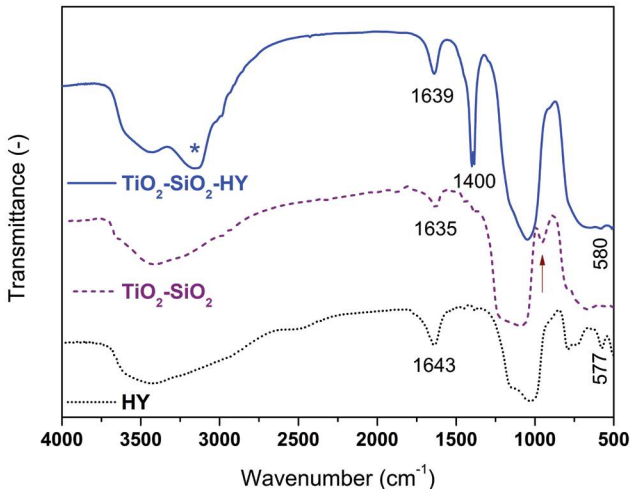

Fig. 3. FTIR spectrum for the HY zeolite and for the prepared composites.

These values suggest that the TiO_2 nanoparticles can anchor only on the surface of the HY zeolite particles.

Surface morphology (acquired by SEM) of cotton textiles after the functionalization process is shown in Fig. 5 (top). As can be observed, the cotton fibers became better coated with the TiO_2 nanoparticles than by the synthesized photocatalysts. Moreover, the composite prepared with the HY zeolite presented a very poor adhesion on the fibers, as already referred in previous work [48]. This behavior can be related to the formation of the agglomerates in the TiO_2-SiO_2-HY composite, so that the bonds between the fiber and composite particles may not be intense enough to overcome their weight. Fig. 5 allows to estimate that the aggregate size (TiO_2-SiO_2-HY photocatalyst) is in the order of 10 μm, that is, about 25 times the average size of HY particles. In this same figure, it is even possible to observe several of these HY particles covered by TiO_2 nanoparticles, forming, in fact, a large cluster. This feature of the HY zeolite in forming clusters can be explained in terms of the charges present in its structure, which facilitate the link between the zeolite and other particles dispersed in the medium during the synthesis process.

Analysis of the chemical composition of the coated cotton textiles was performed via the EDX analysis (Fig. 5), where the information refers to the chemical elements present

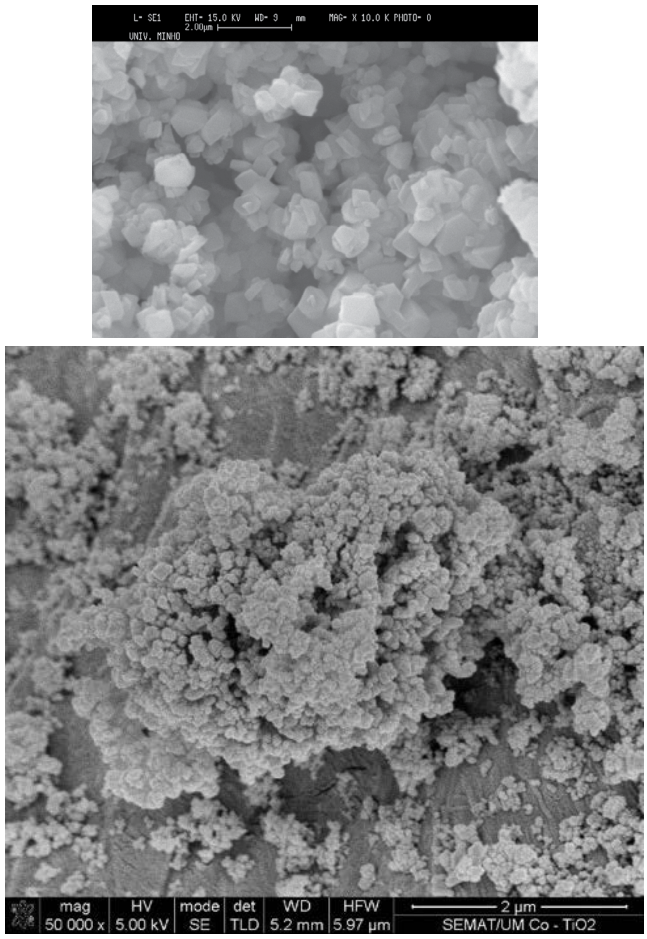

Fig. 4. SEM images of HY zeolite (top) and TiO_2 nanoparticles (bottom).

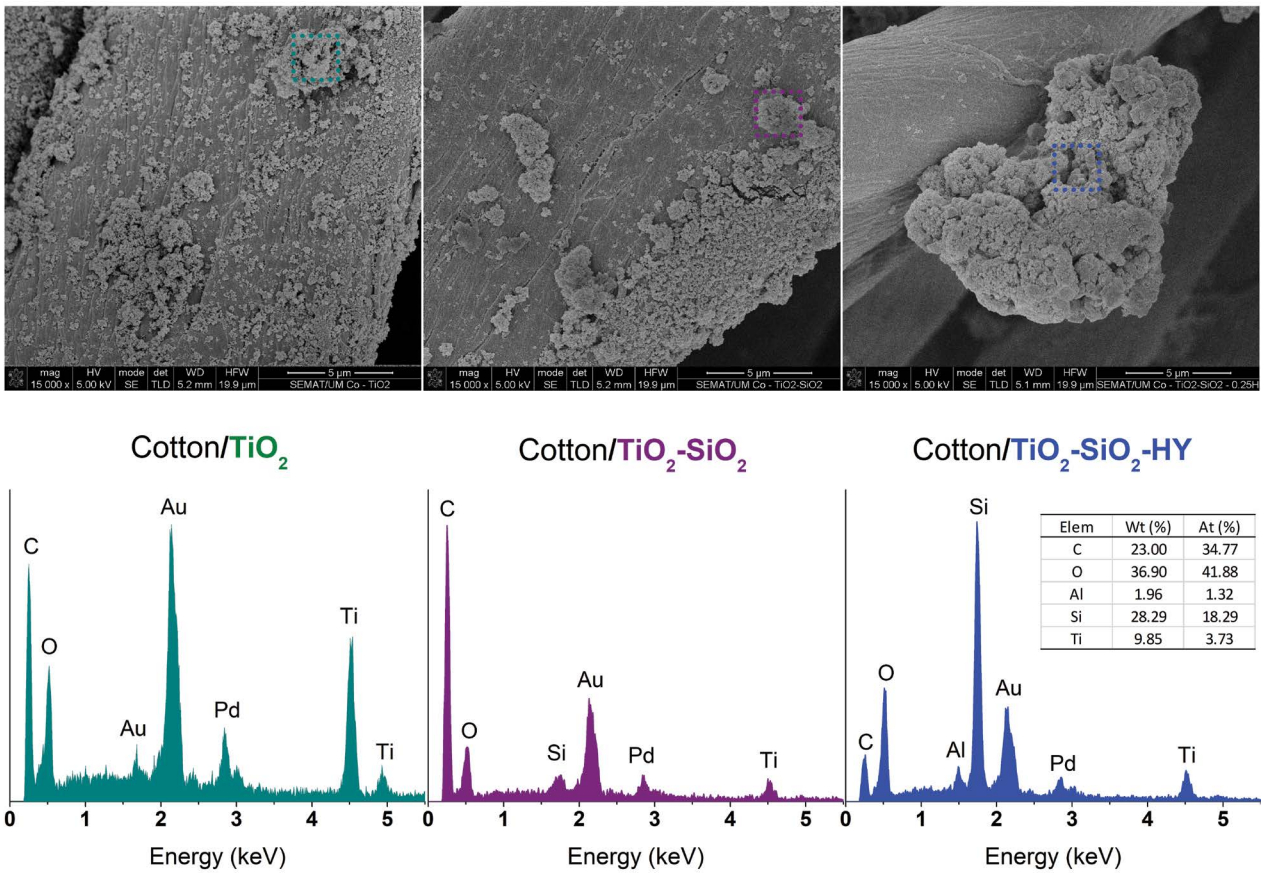

Fig. 5. SEM micrographs for different photocatalysts over cotton textile at magnification 15,000x. Underneath each SEM micrograph, the corresponding EDX spectrum is shown.

in the regions that appear highlighted by a square in the SEM micrographs of the fibers shown at the top of Fig. 5. In the EDX spectra of all samples, the presence of the Ti Kα peak can be highlighted while the Kβ peak is only evident for the cotton/TiO_2 sample (left spectrum in Fig. 5). On the other hand, the peak-related area value of Al and Si atoms for the TiO_2-SiO_2-HY composite indicated in the last column (table inserted in Fig. 5), yields a Si/Al ratio (18.29/1.32 = 13.9) much higher than the value of zeolite HY (2.81). Thus, EDX and SEM analyses confirm the synthesis of a composite based on the HY zeolite impregnated with TiO_2 nanoparticles, in which the SiO_2 has acted as a binder between these materials, as illustrated in Fig. 6.

As can be observed in Table 1, the nitrogen adsorption-desorption equilibrium isotherms reveal a higher surface area as well as total microporous volume (V_{micro}) of the TiO_2-SiO_2-HY composite in comparison with SiO_2, TiO_2 and TiO_2-SiO_2 materials, which is related to the textural properties of HY zeolite [48]. A lower microporosity for TiO_2-SiO_2 composite compared to the TiO_2-SiO_2-HY was observed, which can be related to the mesoporous nature of the SiO_2 and TiO_2 materials. In addition, the substantial increase of the mesopore surface area (S_{meso}) for TiO_2-SiO_2-HY suggest the impregnation of the TiO_2-SiO_2 on the surface of the zeolite during the synthesis process of this composite, as described in Fig. 6.

Fig. 7 presents the zeta potential values for the photocatalysts in aqueous suspension as a function of pH. As can be observed, the TiO_2 nanoparticles exhibited a point of zero charge (PZC) around pH = 5, reflecting the effect of the mixture of anatase and rutile phases [49]. Otherwise, the zeta potential for the TiO_2-SiO_2 and TiO_2-SiO_2-HY composites remained at negative values throughout the analyzed pH range, indicating that in aqueous suspension both synthesized photocatalysts tend to acquire a negative surface charge. The origin of this behavior on the TiO_2-SiO_2 composite can be explained by the presence of a large amount of silanol groups (Si–OH) on the silica surface, which acts as an acid causing a negative surface charge [1]. In the case of TiO_2-SiO_2-HY composite and in according Kuzniatsova et al. [50], the hydroxide groups (Al–OH–Si) on the surface of HY zeolite can de-protonated to form Si–O^- at a large pH range making their surface more negatively charged. The observed differences in electrokinetic behaviors most likely influence the photocatalytic efficiency of these photocatalysts.

From the calibration curve of dye solution (data not shown), that is, absorbance (A) values as a function of dye solution concentration (C or [dye]), it is possible to verify a linear relationship between these parameters (Lambert–Beer law). In simple terms, the concentration of the dye solution in relation to its initial value (C/C_0) was monitored

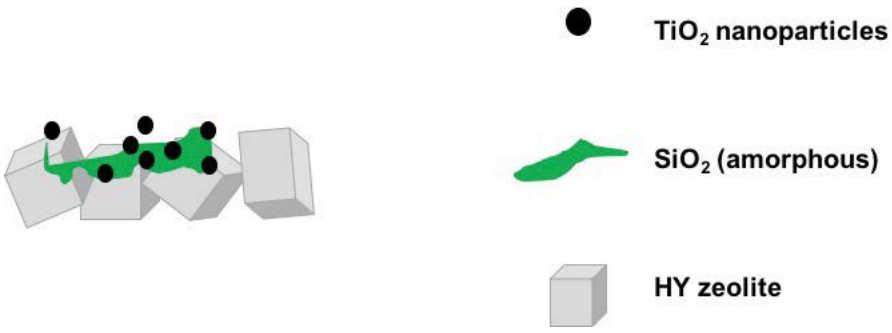

Fig. 6. The suggested relative position of the HY zeolite, SiO_2 and TiO_2 materials after the synthesized composite.

Table 1
Physical properties of the pristine and composite materials

Sample	S_{BET} (m^2/g)	S_{meso} (m^2/g)	V_{micro} (cm^3/g)
SiO_2 [47]	28	30	0
TiO_2 [48]	41	41	0
TiO_2-SiO_2	50	47	0.001
HY [48]	665	25	0.302
TiO_2-SiO_2-HY	465	290	0.050

at specific time intervals from its respective absorbance ratio (A/A_0). Figs. 8a and b show the C/C_0 (C) values during the adsorption (photocatalytic degradation) process for the RhB dye solution treated with pristine and coated cotton textiles.

The decrease of the C/C_0 ratio for cotton/TiO_2 and cotton/TiO_2-SiO_2 samples was notably higher, varying from 1 to about 0.6 after 1 h in the dark (Fig. 8a). The sample cotton/TiO_2-SiO_2 shows a good adsorbability to the RhB molecule, which can probably be attributed to the increased surface area due to the presence of silica, according to Table 1 and published data [47,48,51–53]. On the other hand, despite the large surface area of the HY zeolite (Table 1), its cavities are inaccessible because the size of the RhB molecule is larger than the pore aperture of this HY zeolite [47], which can explain the low adsorption ability of the cotton/HY and cotton/TiO_2-SiO_2-HY samples.

The decrease of the (RhB) after 3 h of irradiation for the solution treated with pristine cotton can be attributed to photolysis and eventually superoxide radicals formed due to the adsorbed O_2 on the cotton fibers. This can also be true for samples of cotton/SiO_2 and cotton/HY. In addition, the presence of acid sites in the HY zeolite can contribute to the degradation of the RhB molecules. Nevertheless, the photocatalytic efficiency of the cotton/TiO_2 sample was the largest among the coated cotton textiles, showing that the combination of SiO_2 with TiO_2 or SiO_2 with HY and TiO_2 does not always form a more efficient photocatalyst than bare TiO_2, in the scope of cotton textiles functionalization. These results can be explained by the excellent anchorage degree of TiO_2 on cotton fibers, contrary to the TiO_2-SiO_2 and TiO_2-SiO_2-HY photocatalysts, as mentioned in the SEM results.

Based on these results, it is important to compare the efficiency of cotton/TiO_2-SiO_2-HY and cotton/TiO_2 samples. Since several studies have shown that the pH of the dye solution plays an important role in the photocatalysis reactions, the effect of the initial pH of RhB solution was studied, by adding NaCl or NaOH, to observe the photocatalytic behavior of the cotton/TiO_2-SiO_2-HY sample (Fig. 9). In this context, the best result was achieved for acidic conditions (pH = 2.7), but even so, the attained performance in terms of RhB dye removal was not as high as that presented by the cotton/TiO_2 sample (Fig. 8). It is known that at pH values higher than pK_a of RhB (3.7), the carboxyl group of the cationic form (Fig. 1) is deprotonated and the RhB molecules also acquire a negative local charge [54]. This hinders the RhB adsorption on the cotton/TiO_2-SiO_2-HY sample (Fig. 9a) due to the TiO_2-SiO_2-HY photocatalyst present a negative surface charge for the pH varying between 2 and 10 (without a PZC), as verified by zeta potential measurements (Fig. 7). Consequently, photocatalytic degradation of the RhB dye may also be hindered. On the other hand, when using a pH lower than the pK_a of RhB (for example 2.7, Fig. 9), the dye and TiO_2-SiO_2-HY composite present opposite surface charges. Therefore, the adsorption of the RhB molecules on the TiO_2-SiO_2-HY composite is favored, which may be related to the best results illustrated in Fig. 9 (curve with stars).

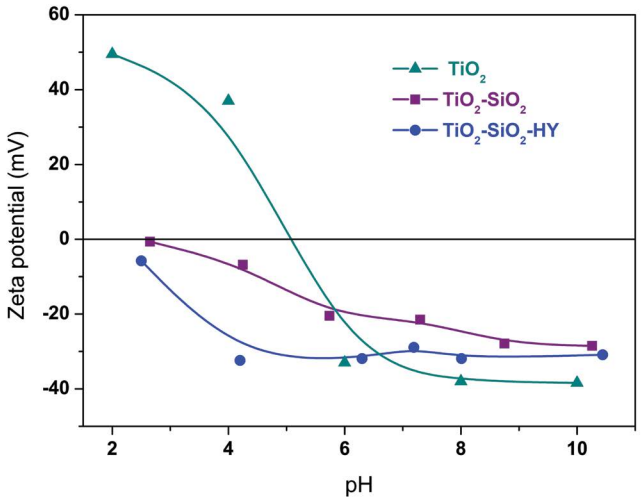

Fig. 7. Zeta potential vs. pH curves of the photocatalysts in aqueous suspension.

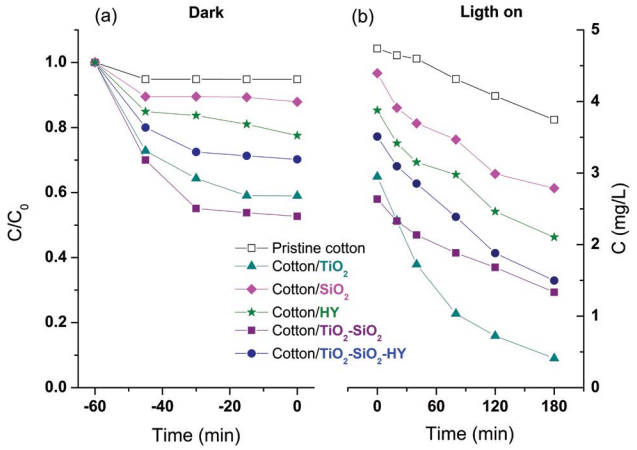

Fig. 8. Decrease of RhB dye solution concentration due to the adsorption in the dark (a) and photocatalytic degradation (b) under similar solar irradiation. Experimental conditions: 35°C; initial pH = 5.9; C_0 (RhB) = 5.0 mg/L.

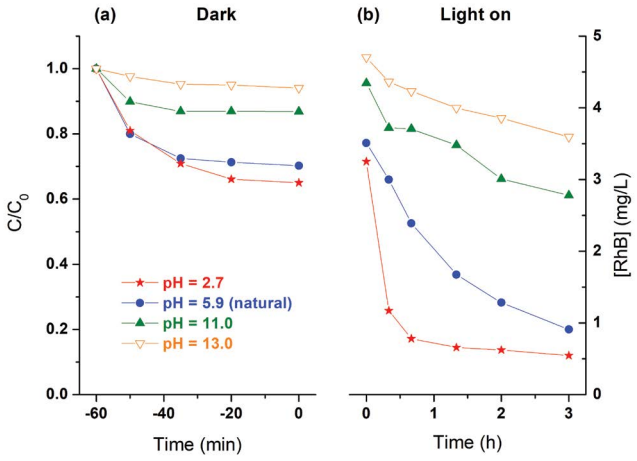

Fig. 9. Decrease of RhB dye solution concentration at different initial pH values treated with the cotton/TiO_2-SiO_2-HY sample. Experimental conditions: 35°C; C_0 (RhB) = 5.0 mg/L.

Besides the RhB dye, it was also studied the photocatalytic degradation of RR120 dye solution. From Fig. 10, it can be observed that all samples showed a similar behavior under dark conditions. It is important to note that the structure of the RR120 dye molecule is much larger than that of RhB dye (Fig. 1) and is of greater complexity. Thus, it is likely that RR120 molecules do not have easy access to the inner regions of the photocatalysts, but only to the outer surface of the cotton fibers. If so, all samples really should have a similar tendency for the adsorption of RR120 dye. After the irradiation process, the slight increase observed in the C/C_0 values, except for the cotton/TiO_2 sample, corroborates this hypothesis. Since the increase in temperature from the instant the lamp is turned on results in the desorption of the RR120 molecules on the cotton fibers and, consequently, their dissolution into the aqueous solution, then an increase in the RR120 dye concentration occurs.

Fig. 8 also shows that the ability of the analyzed samples to degrade the RR120 dye solution is markedly different,

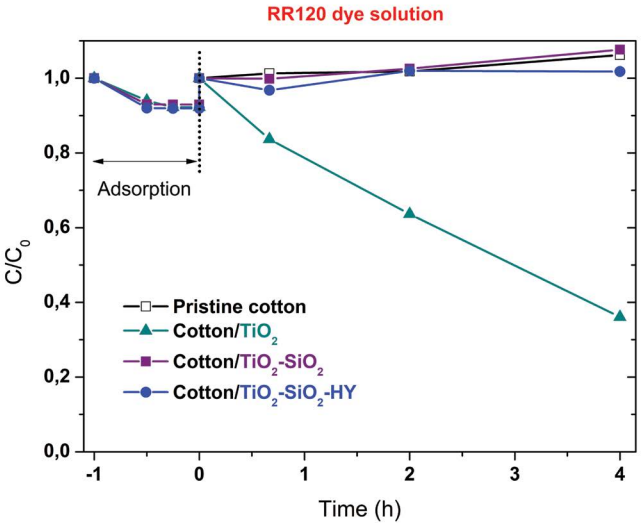

Fig. 10. Variation of RR120 dye solution concentration treated with different samples. Experimental conditions: 35°C; initial pH = 4.5; C_0 (RR120) = 25 mg/L.

as the cotton/TiO_2 sample was the only one that presented photocatalytic capacity. This behavior may be related to the nature of the photocatalyst's surface charges in an aqueous solution. The zeta potential measurements suggest a very poor adsorbability of TiO_2-SiO_2 and TiO_2-SiO_2-HY photocatalysts for anionic species, such as the RR120 dye, which may explain the absence of a decrease in the C/C_0 values. In contrast, the TiO_2 nanoparticles showed a positive surface charge at pH < 5, suggesting good adsorption of RR120 molecules and also efficient photocatalytic degradability under UV light, as TiO_2 nanoparticles also showed bandgap energy equal to 3.19 eV (389 nm) [48]. However, additional essays varying the initial pH of RR120 dye aqueous solution are required to test this hypothesis.

4. Conclusion

In this work, the self-cleaning property of the diverse photocatalytic samples that were produced was evaluated by the discoloration of RhB and RR120 dyes in an aqueous solution under simulated sunlight irradiation. Based on the experimental results, the following conclusions can be made:

- SEM micrographs showed that the cotton fibers were better coated with TiO_2 nanoparticles, while the TiO_2-SiO_2-HY composite only presented poor adhesion on the fibers;
- The addition of SiO_2 to TiO_2 framework enhanced the adsorption of RhB molecules, probably due to the increase in surface area. However, the low percentage of the photocatalyst had no synergistic effect on the photocatalytic property of cotton textile coated with this composite;
- The photocatalytic efficiency of the cotton/TiO_2 sample was higher than that found for cotton/TiO_2-SiO_2 and cotton/TiO_2-SiO_2-HY, suggesting that, in this case,

the fixation degree of the photocatalysts on cotton textiles may be the key for RhB degradation;
- Under alkaline conditions, there was a decrease in the photocatalytic activity of the cotton/TiO_2-SiO_2-HY sample in relation to the degradation of the RhB dye, as in these experimental conditions the RhB molecules acquire a negative local charge, resulting in repulsive forces between the photocatalyst and dye, which therefore tend to separate them further from each other;
- All the functionalized textiles showed similar adsorbability for the RR120 dye, suggesting that the adsorption process of this molecule occurs merely on the external surface of the composites and on the cotton fibers. On the other hand, only the cotton/TiO_2 sample showed the ability to photodegrade the RR120 dye, probably because except for the case of TiO_2, the increase of temperature after the lamp activation caused a desorption of the RR120 molecules on the composite surfaces.

Acknowledgments

Salmon Landi Jr. thanks the Capes/Brazil for supports his Doctoral Fellowship (13346/13-0). The authors are also grateful to the financial support of the project "AIProcMat@N2020-Advanced Industrial Processes and Materials for a Sustainable Northern Region of Portugal 2020", with the reference NORTE-01-0145-FEDER-000006 and the project BioTecNorte (operation NORTE-01-0145-FEDER-000004), supported by Norte Portugal Regional Operational Programme (NORTE 2020), under the Portugal 2020 Partnership Agreement, through the European Regional Development Fund (ERDF). This work also has been funded by ERDF through COMPETE2020-Programa Operacional Competitividade e Internacionalização (POCI), Project POCI-01-0145-FEDER-006984 – Associate Laboratory LSRE-LCM and by Portuguese funds through FCT-Fundação para a Ciência e a Tecnologia under the Strategic Funding UID/FIS/04650/2019 as well as project PTDC/AAGTEC/5269/2014 and Centre of Chemistry (UID/QUI/00686/2013 and UID/QUI/0686/2016).

References

[1] J. Schneider, M. Matsuoka, M. Takeuchi, J.L. Zhang, Y. Horiuchi, M. Anpo, D.W. Bahnemann, Understanding TiO_2 photocatalysis: mechanisms and materials, Chem. Rev., 114 (2014) 9919–9986.
[2] M.J. Hernández Rodríguez, E. Pulido Melián, O. González Díaz, J. Araña, M. Macías, A. González Orive, J.M. Doña Rodríguez, Comparison of supported TiO_2 catalysts in the photocatalytic degradation of NO_x, J. Mol. Catal. A: Chem., 413 (2016) 56–66.
[3] B.M. Pirzada, N.A. Mir, N. Qutub, O. Mehraj, S. Sabir, M. Muneer, Synthesis, characterization and optimization of photocatalytic activity of TiO_2/ZrO_2 nanocomposite heterostructures, Mater. Sci. Eng. B, 193 (2015) 137–145.
[4] F.Z. Li, J.S. Zhou, C. Du, W. Li, Y.Z. Wang, G.N. He, Q.Y. He, Preparation and photocatalytic properties of porous C and N co-doped TiO_2 deposited on brick by a fast, one-step microwave irradiation method, J. Environ. Sci., 60 (2017) 24–32.
[5] S. Silvestri, B. Hennemann, N. Zanatta, E.L. Foletto, Photocatalytic efficiency of TiO_2 supported on raw red clay disks to discolour Reactive red 141, Water Air Soil Pollut., 229 (2018) doi: 10.1007/s11270-018-3700-x.
[6] R. Zouzelka, J. Rathousky, Photocatalytic abatement of NO_x pollutants in the air using commercial functional coating with porous morphology, Appl. Catal., B, 217 (2017) 466–476.
[7] M. Faraldos, A. Bahamonde, Environmental applications of titania-graphene photocatalysts, Catal. Today, 285 (2017) 13–28.
[8] N. Chekir, O. Benhabiles, D. Tassalit, N.A. Laoufi, F. Bentahar, Photocatalytic degradation of methylene blue in aqueous suspensions using TiO_2 and ZnO, Desal. Water Treat., 57 (2016) 6141–6147.
[9] K.E. O'Shea, D.D. Dionysiou, Advanced oxidation processes for water treatment, J. Phys. Chem. Lett., 3 (2012) 2112–2113.
[10] A. Buthiyappan, A.R. Abdul Aziz, W.M.A. Wan Daud, Recent advances and prospects of catalytic advanced oxidation process in treating textile effluents, Rev. Chem. Eng., 32 (2016) 1–47, doi: 10.1515/revce-2015-0034.
[11] F. Harrelkas, A. Paulo, M.M. Alves, L. El Khadir, O. Zahraa, M.N. Pons, F.P. van der Zee, Photocatalytic and combined anaerobic–photocatalytic treatment of textile dyes, Chemosphere, 72 (2008) 1816–1822.
[12] Z.-A. Mirian, A. Nezamzadeh-Ejhieh, Removal of phenol content of an industrial wastewater via a heterogeneous photodegradation process using supported FeO onto nanoparticles of Iranian clinoptilolite, Desal. Water Treat., 57 (2016) 16483–16494.
[13] M.D. Hernández-Alonso, F. Fresno, S. Suárez, J.M. Coronado, Development of alternative photocatalysts to TiO_2: Challenges and opportunities, Energy Environ. Sci., 2 (2009) 1231–1257.
[14] A.F. Khan, M. Mehmood, S.K. Durrani, M.L. Ali, N.A. Rahim, Structural and optoelectronic properties of nanostructured TiO_2 thin films with annealing, Mater. Sci. Semicond. Process, 29 (2015) 161–169.
[15] M. Antonopoulou, E. Evgenidou, D. Lambropoulou, I. Konstantinou, A review on advanced oxidation processes for the removal of taste and odor compounds from aqueous media, Water Res., 53 (2014) 215–234.
[16] J.O. Tijani, O.O. Fatoba, G. Madzivire, L.F. Petrik, A review of combined advanced oxidation technologies for the removal of organic pollutants from water, Water Air Soil Pollut., 225 (2014), doi: 10.1007/s11270-014-2102-y.
[17] M.N. Chong, B. Jin, C.W.K. Chow, C. Saint, Recent developments in photocatalytic water treatment technology: a review, Water Res., 44 (2010) 2997–3027.
[18] M. Faraldos, R. Kropp, M.A. Anderson, K. Sobolev, Photocatalytic hydrophobic concrete coatings to combat air pollution, Catal. Today, 259 (2016) 228–236.
[19] A. Mills, S. Elouali, The nitric oxide ISO photocatalytic reactor system: measurement of NO_x removal activity and capacity, J. Photochem. Photobiol., A, 305 (2015) 29–36.
[20] F. Chen, J. Zhao, H. Hidaka, Highly selective deethylation of Rhodamine B: adsorption and photooxidation pathways of the dye on the TiO_2/SiO_2 composite photocatalyst, Int. J. Photoenergy, 5 (2003) 209–217.
[21] D.M. Tobaldi, R.C. Pullar, A.F. Gualtieri, G. Otero-Irurueta, M.K. Singh, M.P. Seabra, J.A. Labrincha, Nitrogen-modified nano-titania: true phase composition, microstructure and visible-light induced photocatalytic NO_x abatement, J. Solid State Chem., 231 (2015) 87–100.
[22] B. Dai, M. Xuan, Y.H. Lv, C.G. Jin, S.L. Ran, Molten salt synthesis of Bi_2WO_6 powders and its visible-light photocatalytic activity, Mater. Res., 22 (2019), doi: 10.1590/1980-5373-MR-2019-0311.
[23] R. Daghrir, P. Drogui, D. Robert, Modified TiO_2 for environmental photocatalytic applications: a review, Ind. Eng. Chem. Res., 52 (2013) 3581–3599.
[24] K. Bourikas, C. Kordulis, A. Lycourghiotis, Titanium dioxide (anatase and rutile): surface chemistry, liquid–solid interface chemistry, and scientific synthesis of supported catalysts, Chem. Rev., 114 (2014) 9754–9823.
[25] A. Fujishima, T.N. Rao, D.A. Tryk, Titanium dioxide photocatalysis, J. Photochem. Photobiol., C, 1 (2000) 1–21.
[26] E. Pakdel, W.A. Daoud, Self-cleaning cotton functionalized with TiO_2/SiO_2: focus on the role of silica, J. Colloid Interface Sci., 401 (2013) 1–7.

[27] I. Levchuk, M. Sillanpää, C. Guillard, D. Gregori, D. Chateau, S. Parola, TiO_2/SiO_2 porous composite thin films: role of TiO_2 areal loading and modification with gold nanospheres on the photocatalytic activity, Appl. Surf. Sci., 383 (2016) 367–374.
[28] T. Yuranova, R. Mosteo, J. Bandara, D. Laub, J. Kiwi, Self-cleaning cotton textiles surfaces modified by photoactive SiO_2/TiO_2 coating, J. Mol. Catal. A: Chem., 244 (2006) 160–167.
[29] M. Momeni, H. Saghafian, F. Golestani-Fard, N. Barati, A. Khanahmadi, Effect of SiO_2 addition on photocatalytic activity, water contact angle and mechanical stability of visible light activated TiO_2 thin films applied on stainless steel by a sol gel method, Appl. Surf. Sci., 392 (2017) 80–87.
[30] U. Diebold, The surface science of titanium dioxide, Surf. Sci. Rep., 48 (2003) 53–229.
[31] L.D. Borges, J.L. de Macedo, Solid-state dealumination of zeolite Y: structural characterization and acidity analysis by calorimetric measurements, Microporous Mesoporous Mater., 236 (2016) 85–93.
[32] J. Esmaili-Hafshejani, A. Nezamzadeh-Ejhieh, Increased photocatalytic activity of Zn(II)/Cu(II) oxides and sulfides by coupling and supporting them onto clinoptilolite nanoparticles in the degradation of benzophenone aqueous solution, J. Hazard. Mater., 316 (2016) 194–203.
[33] A. Corma, H. Garcia, Supramolecular host-guest systems in zeolites prepared by ship-in-a-bottle synthesis, Eur. J. Inorg. Chem., 2004 (2004) 1143–1164.
[34] J.O. Carneiro, S. Azevedo, F. Fernandes, E. Freitas, M. Pereira, C.J. Tavares, S. Lanceros-Méndez, V. Teixeira, Synthesis of iron-doped TiO_2 nanoparticles by ball-milling process: the influence of process parameters on the structural, optical, magnetic, and photocatalytic properties, J. Mater. Sci., 49 (2014) 7476–7488.
[35] M. Neamtu, A. Yediler, I. Siminiceanu, A. Kettrup, Oxidation of commercial reactive azo dye aqueous solutions by the photo-Fenton and Fenton-like processes, J. Photochem. Photobiol., A, 161 (2003) 87–93.
[36] R. Díaz, S. Macías, E. Cázares, Fourier transform infrared spectroscopy and atomic force microscopy studies of a SiO_2-TiO_2-zeolite matrix for a CuO-CoO catalyst prepared by a sol–gel method, J. Sol–Gel Sci. Technol., 35 (2005) 13–20.
[37] B. Xu, J. Ding, L. Feng, Y.Y. Ding, F.Y. Ge, Z.S. Cai, Self-cleaning cotton fabrics via combination of photocatalytic TiO_2 and superhydrophobic SiO_2, Surf. Coat. Technol., 262 (2015) 70–76.
[38] D.S.S. Padovini, A.G. Magdalena, R.G. Capeli, E. Longo, C.J. Dalmaschio, A.J. Chiquito, F.M. Pontes, Synthesis and characterization of $ZrO_2@SiO_2$ core-shell nanostructure as nanocatalyst: application for environmental remediation of Rhodamine B dye aqueous solution, Mater. Chem. Phys., 233 (2019) 1–8.
[39] A.C. Lopes, M.P. Silva, R. Gonçalves, M.F.R. Pereira, G. Botelho, A.M. Fonseca, S. Lanceros-Mendez, I.C. Neves, Enhancement of the dielectric constant and thermal properties of α-poly(vinylidene fluoride)/zeolite nanocomposites, J. Phys. Chem. C, 114 (2010) 14446–14452.
[40] J.A. Kaduk, J. Faber, Crystal structure of zeolite Y as a function of ion exchange, Rigaku J., 12 (1995) 14–34.
[41] I.C. Neves, G. Botelho, A.V. Machado, P. Rebelo, Catalytic degradation of polyethylene: an evaluation of the effect of dealuminated Y zeolites using thermal analysis, Mater. Chem. Phys., 104 (2007) 5–9.
[42] W. Lutz, C.H. Rüscher, D. Heidemann, Determination of the framework and non-framework $[SiO_2]$ and $[AlO_2]$ species of steamed and leached faujasite type zeolites: calibration of IR, NMR, and XRD data by chemical methods, Microporous Mesoporous Mater., 55 (2002) 193–202.
[43] A. Nezamzadeh-Ejhieh, E. Shahriari, Photocatalytic decolorization of methyl green using Fe(II)-o-phenanthroline as supported onto zeolite Y, J. Ind. Eng. Chem., 20 (2014) 2719–2726.
[44] R. Díaz, J. Cruz, R. Ocampo, Fourier transform infrared spectroscopic comparison of Cu, Co/Si-Al-Zeolite catalysts prepared by a combined sol–gel method, Langmuir, 13 (1997) 6861–6863.
[45] A. Nezamzadeh-Ejhieh, M. Bahrami, Investigation of the photocatalytic activity of supported ZnO–TiO_2 on clinoptilolite nano-particles towards photodegradation of wastewater-contained phenol, Desal. Water Treat., 55 (2015) 1096–1104.
[46] M. Bahrami, A. Nezamzadeh-Ejhieh, Effect of supporting and hybridizing of FeO and ZnO semiconductors onto an Iranian clinoptilolite nano-particles and the effect of ZnO/FeO ratio in the solar photodegradation of fish ponds waste water, Mater. Sci. Semicond. Process., 27 (2014) 833–840.
[47] S. Landi Jr., J. Carneiro, S. Ferdov, A.M. Fonseca, I.C. Neves, M. Ferreira, P. Parpot, O.S.G.P. Soares, M.F.R. Pereira, Photocatalytic degradation of Rhodamine B dye by cotton textile coated with SiO_2-TiO_2 and SiO_2-TiO_2-HY composites, J. Photochem. Photobiol., A, 346 (2017) 60–69.
[48] S. Landi Jr., J. Carneiro, O.S.G.P. Soares, M.F.R. Pereira, A.C. Gomes, A. Ribeiro, A.M. Fonseca, P. Parpot, I.C. Neves, Photocatalytic performance of N-doped TiO_2 nano-SiO_2-HY nanocomposites immobilized over cotton fabrics, J. Mater. Res. Technol., 8 (2019) 1933–1943.
[49] S. Landi Jr., J.O. Carneiro, F. Fernandes, P. Parpot, J. Molina, F. Cases, J. Fernández, J.G. Santos, G.M.B. Soares, V. Teixeira, A.P. Samantilleke, Functionalization of cotton by RGO/TiO_2 to enhance photodegradation of Rhodamine B under simulated solar irradiation, Water Air Soil Pollut., 228 (2017) 335, 10.1007/s11270-017-3533-z.
[50] T. Kuzniatsova, Y.H. Kim, K. Shqau, P.K. Dutta, H. Verweij, Zeta potential measurements of zeolite Y: application in homogeneous deposition of particle coatings, Microporous Mesoporous Mater., 103 (2007) 102–107.
[51] S.G. Kumar, L.G. Devi, Review on modified TiO_2 photocatalysis under UV/Visible light: selected results and related mechanisms on interfacial charge carrier transfer dynamics, Phys. Chem. A, 115 (2011) 13211–13241.
[52] C. Shifu, C. Gengyu, The effect of different preparation conditions on the photocatalytic activity of TiO_2·SiO_2/beads, Surf. Coat. Technol., 200 (2006) 3637–3643.
[53] A. Mahyar, M.A. Behnajady, N. Modirshahla, Characterization and photocatalytic activity of SiO_2-TiO_2 mixed oxide nanoparticles prepared by sol-gel method, Indian J. Chem., 49A (2010) 1593–1600.
[54] S. Merouani, O. Hamdaoui, F. Saoudi, M. Chiha, Sonochemical degradation of Rhodamine B in aqueous phase: effects of additives, Chem. Eng. J., 158 (2010) 550–557.